

Quasimolecular-state interference studies: Collisions between ions ranging from Li^+ to Al^+ and Ne atoms

T. Andersen, A. Kirkegaard Nielsen, and K. J. Olsen

Institute of Physics, University of Aarhus, DK-8000 Aarhus C, Denmark

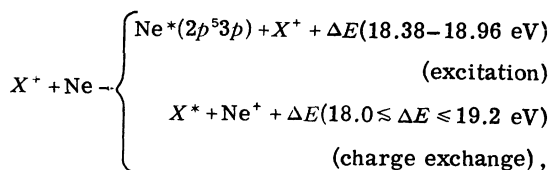
(Received 1 April 1974)

A systematic investigation of the interference of energetically neighboring quasimolecular terms giving rise to oscillatory structure in the total cross sections for diabatic processes has been performed by optical studies of selected spectral lines produced in ion-atom collisions. All ions ranging from Li^+ to Al^+ have been used as projectiles with energies varying from 0.1 to 15 keV using Ne as the target. Interference between direct-excitation and charge-exchange collision channels leading to regularly spaced oscillations which are 180° out of phase have been seen in the N^+ -Ne, O^+ -Ne, Na^+ -Ne, and Mg^+ -Ne systems. The behavior of the oscillations present in the total emission cross sections for the $3p$ levels in Ne cannot be accounted for by the theoretical predictions of Ankudinov *et al.* Strong polarization effects have been seen in the optical radiation from the $3p' \left[\frac{3}{2} \right]_1$ level in Ne in all systems and for the $3p \ ^1P_1$ level in Mg in the Mg^+ -Ne system. The oscillations in the Ne excitation function are mainly due to the polarization component of the radiation perpendicular to the beam direction for the N^+ -Ne, O^+ -Ne, and Na^+ -Ne systems, whereas the parallel component also plays a dominant role in the Mg^+ -Ne system. The molecular-orbital (MO) model is used to account for the polarization data.

During recent years, low-energy ion-atom and ion-molecule collisions have attracted considerable interest since it was established¹ that these collision processes can be highly effective for the production of optical excitation, in contradiction to the well-known "adiabatic criterion."²

Some of these low-energy ion-atom systems exhibit a common feature of interest. The excitation functions depend in a regular oscillatory way on the inverse velocity v^{-1} of the incident ion.³ The cross section for the charge exchange of the incident ion, leading either to the ground state or to an excited state in the corresponding atom, has also been observed to show regular oscillations. These oscillations are alike in spacing, but are in antiphase with the oscillations present in the direct-excitation cross section for the target gas.^{3,4}

The present paper reports on a systematic investigation of low-energy collisions between singly ionized ions, ranging from Li^+ to Al^+ ; and Ne atoms according to the following reaction scheme:



with the purpose of gaining information about the criteria for obtaining a regular oscillatory struc-

ture in the total excitation cross sections. So far, the oscillatory structure in the total excitation or charge-exchange cross sections due to interference between near-degenerate energy levels in the pseudomolecules⁵ has been reported mainly for alkali-ion,^{3,4} alkali-atom,⁶ or inert-gas-ion^{3,4} interactions with the inert gases.

The systems chosen make it possible to perform investigations of the polarization of the light emitted from the interacting particles. Polarization measurements may give detailed information on the pseudomolecular-level systems responsible for the observed oscillatory behavior of the total excitation and charge-exchange cross sections.

Preliminary results from this study have already been reported,⁷ indicating that interference between direct excitation and charge-exchange collision channels occurs for some of the investigated systems. Strong polarization effects were observed for the optical radiation emitted from excited states in Ne, in particular for the Na^+ -Ne and O^+ -Ne systems. Tolk *et al.*⁸ have reported similar polarization effects for the Na^+ -Ne system and explained the observed oscillations in the total cross section and the polarization data as being due exclusively to a selective electron population of the $5f\sigma-4d\sigma$ interfering molecular orbitals in the $(\text{NaNe})^+$ pseudomolecule.

In the present paper, detailed data on the investigated systems are presented together with an analysis of the polarization data. For the Na^+ -Ne system, the interpretation does not support the conclusions reached by Tolk *et al.*⁸

I. EXPERIMENTAL

A. Apparatus

For the production of a beam of Li^+ , Be^+ , B^+ , C^+ , N^+ , O^+ , F^+ , Ne^+ , Na^+ , Mg^+ , or Al^+ ions in the energy range from 50 to 15 keV, the low-energy electromagnetic ion accelerator at Aarhus University was used. It is equipped with a universal ion source,⁹ an extraction electrode, an electrostatic lens system, and an analyzing magnet. Gases were used as source material for C, N, O, and Ne. Source materials and operation parameters for the other beams are described in Ref. 10. The accelerator is equipped with three acceleration-power supplies (0–15 kV, 0–2 kV, and 0–300 V) to obtain a good determination of the beam energy, the uncertainty of which is 1.5 parts per 1000 of the maximum voltage of the power supply used. Ion currents ranging from $\sim 100 \mu\text{A}$ at 15 kV to $\sim 100 \text{nA}$ at 100 V were obtained. Experiments with ^{24}Mg , ^{25}Mg , and ^{26}Mg isotopes showed that the mass separation met the demands for the present experiments, and no contamination of the beams was observed.

The beam traversed a pumping chamber and entered the target chamber through a set of collimators, 1.5 mm in diameter and placed 10 cm apart. The position of the entrance slit can be changed so that it is possible to vary the path length through the gas before the observation region; this is useful for investigating the influence of the finite lifetime of the level of the excited beam particles on the radiation process. The beam current was measured in a Faraday cup.

The target gas Ne was brought into the collision chamber via a needle valve. It flowed via a collimator into the pumping chamber, where it was pumped away by means of an oil-diffusion pump. The pressure in the target chamber was about 500 times greater than that in the pumping chamber. The gas pressure in the collision chamber ranged from 2×10^{-4} to 2.6×10^{-3} Torr. Below $\sim 10^{-3}$ Torr, the demands for a single-collision region were fulfilled. When it was necessary to carry out measurements at pressures higher than $\sim 10^{-3}$ Torr because of low light intensity, corrections were made, so the intensity data were comparable with the results obtained in the single-collision region. The gas pressure in the collision chamber was measured with a Pirani gauge placed very close to the observation region.

The radiation produced by the excited beam and the target particles was measured by means of a 0.3-m McPherson model-218 spectrometer ($f \approx 5.3$) with a 1200-lines/mm reflecting grating and a blaze angle of 5000 Å. The dispersion was $\sim 26 \text{Å/mm}$. The photons were detected with EMI

photomultipliers cooled to -78°C . For wavelengths between 5600 and 8500 Å, the 9658 B modified S-20 type was used; below 5500 Å, the 6256 S-type was used. EMI magnetic-focusing assemblies, type C122/12, were used to reduce the effective cathode area and obtain a reduced dark current (2 to 3 counts/sec) and an improved signal-to-noise ratio (a factor of 6) in the case of the 9658 B. The monochromator was mounted on the collision chamber at 90° with respect to the beam.

For some measurements below 300 V, the monochromator was replaced by a series of selected narrow-band filters. The sensitivity of the monochromator with photomultipliers was determined by means of a standard-for-spectral-radiation lamp (GE 30A/T24/17, Eppley Lab). A Barocel electric manometer, type 1083, was used for the pressure calibration.

Polarization measurements were performed by means of a Pola-Coat UV-105 polarizer placed in the light path between the collision chamber and the monochromator. The polarizer could be rotated 0 – 90° around the optical axis. The polarizing effect of the reflecting grating of the monochromator has been measured previously.¹¹ Only a small deviation between the previously determined and the present eigenpolarizations of the grating was observed. The polarization fraction $P = (I_{\parallel} - I_{\perp}) / (I_{\parallel} + I_{\perp})$, where I_{\parallel} and I_{\perp} are the intensities with electric vectors parallel and perpendicular to the beam axis, respectively. The total intensity is obtained from the relation $I_{\text{tot}} = \frac{2}{3}(I_{\parallel} + 2I_{\perp})$. If the polarization fraction is larger than 10%, the total intensities are derived from the I_{\parallel} and I_{\perp} components.

B. Total-emission cross sections

The accuracy of the total-emission cross sections stated for some of the systems depends mainly on the calibration of the optical system for which the accuracy of the quantitative efficiency is estimated to be $\pm 30\%$ or larger, depending on the appropriate wavelength. When corrections caused by (i) cascading from higher-lying levels, (ii) the finite lifetime of the excited levels in the projectile atoms, (iii) Doppler effects, and (iv) the application of pressures above the single-collision region are taken into consideration the accuracy of the total cross sections may be determined to be $\pm 50\%$ at energies above 1 keV, but they increase to $\sim \pm 100\%$ at lower energies.

The calibration procedure was tested by measuring a number of total-emission cross sections for He levels such as 3^3S , 3^1D , and 3^3D after He^+ -Ne collisions—previously reported by Wolterbeek Müller and de Heer.¹² In general, the agreement was fair, with deviations of less than 25%.

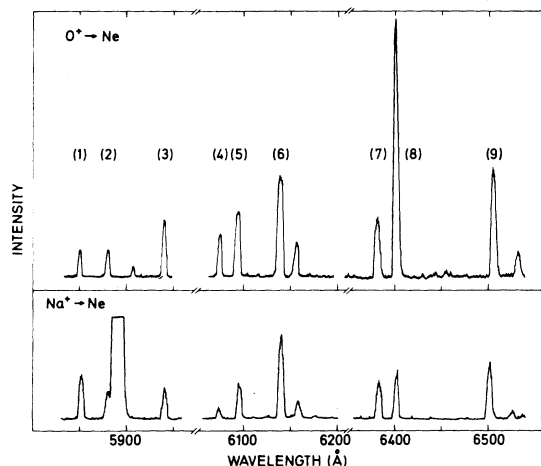


FIG. 1. Partial spectral scans of the wavelength region containing the $3s-3p$ transitions in NeI for the O^+-Ne and Na^+-Ne systems. Same beam current was used for Na^+ and O^+ . Spectral lines marked are (1) 5852 Å ($3p'[\frac{1}{2}]_0$), (2) 5881 Å ($3p'[\frac{1}{2}]_1$), (3) 5944 Å ($3p'[\frac{3}{2}]_2$), (4) 6074 Å ($3p[\frac{1}{2}]_0$), (5) 6096 Å ($3p'[\frac{3}{2}]_2$), (6) 6143 Å ($3p[\frac{3}{2}]_2$), (7) 6382 Å ($3p[\frac{3}{2}]_1$), (8) 6402 Å ($3p[\frac{3}{2}]_3$), (9) 6506 Å ($3p[\frac{5}{2}]_2$), with the upper level given in the bracket.

II. RESULTS

The 11 systems investigated may be divided into two groups according to the excitation functions obtained for the ten $3p$ levels in Ne. The N^+-Ne , O^+-Ne , Na^+-Ne , and Mg^+-Ne systems all exhibit excitation functions with a strong oscillatory dependence on the energy of the projectile. The other collision systems display excitation functions which are either smooth curves or contain oscillations of a nonregular character only.

The spectral distribution investigated for all the

systems within the region 2500–8500 Å showed that the first and second spectra of neon and of the applied projectile could account for the observed spectral lines. In the region of special interest of the $3p$ levels in Ne, the 5600–7600 Å region, approximately 45 spectral lines could be attributed to Ne. Twenty-seven spectral lines with strong intensities could be classified as $3s-3p$ transitions. Cascading population of the $3p$ levels from higher-lying $5s$, $6s$, $3d$, or $4d$ levels could be seen, but in general, the cascading components were 10–100 times weaker than the $3s-3p$ transitions. The $3p[\frac{1}{2}]_1-3d$ spectral lines, which are the strongest cascading transitions observed, have an intensity amounting to $\sim\frac{1}{3}$ the intensity observed for the $3s-3p[\frac{1}{2}]_1$ transitions. Hence population through cascading plays a role for the $3p[\frac{1}{2}]_1$ level, whereas the other nine levels are predominantly populated by direct excitation.

A. Strong oscillatory systems

Partial scans of the wavelength region from 5800–6600 Å are shown in Fig. 1 for the O^+-Ne and the Na^+-Ne systems for projectile energies of 15 keV. A marked difference can be seen in the relative spectral intensities for some of the $3s-3p$ transitions.

In Table I is given a comparison of the sums of the spectral intensities depopulating the ten $3p$ levels in Ne for the four systems, N^+-Ne , O^+-Ne , Na^+-Ne , and Mg^+-Ne , all at a projectile energy of 15 keV. The data are normalized to the $3s[\frac{3}{2}]_2-3p[\frac{3}{2}]_3$ transition at 6402 Å, the only one depopulating the $3p[\frac{3}{2}]_3$ level. Since the Na data differ considerably from the three other systems, a relative comparison is obtained by reducing the original

TABLE I. Sum of the $3s-3p$ spectral-line intensities in NeI.

LS	Upper level		Excitation energy (eV)	N^+-Ne	O^+-Ne	Na^+-Ne	Mg^+-Ne
	Racah	Paschen					
$3p\ ^1S_0$	$3p'[\frac{1}{2}]_0$	$2p_1$	18.96	7	7	50(13)	7
$3p\ ^3P_1$	$3p'[\frac{1}{2}]_1$	$2p_2$	18.72	43	46	185(46)	48
$3p\ ^3P_0$	$3p[\frac{1}{2}]_0$	$2p_3$	18.71	10	11	14(4)	11
$3p\ ^3P_2$	$3p'[\frac{3}{2}]_2$	$2p_4$	18.70	66	68	212(53)	82
$3p\ ^1P_1$	$3p'[\frac{3}{2}]_1$	$2p_5$	18.69	46	46	164(41)	41
$3p\ ^1D_2$	$3p[\frac{3}{2}]_2$	$2p_6$	18.63	66	74	310(77)	82
$3p\ ^3D_1$	$3p[\frac{3}{2}]_1$	$2p_7$	18.61	45	40	108(27)	43
$3p\ ^3D_2$	$3p[\frac{5}{2}]_2$	$2p_8$	18.57	74	71	176(44)	97
$3p\ ^3D_3$	$3p[\frac{5}{2}]_3$	$2p_9$	18.55	100	100	100(25)	100
$3p\ ^3S_1$	$3p[\frac{1}{2}]_1$	$2p_{10}$	18.38	42	38	56(14)	52

data by a factor of 4. These data are given in brackets in Table I. The $3p'[\frac{1}{2}]_0$ level is more populated in the Na^+ -Ne collision system than in N^+ -Ne, O^+ -Ne, or Mg^+ -Ne collisions, whereas the $3p[\frac{1}{2}]_0$, $3p[\frac{5}{2}]_3$, and $3p[\frac{1}{2}]_1$ levels are less populated in the Na^+ -Ne system than in the three other collision systems.

Measurements of the total photon yield from the $3s$ - $3p$ transitions in Ne for the projectiles N^+ , O^+ , Na^+ , and Mg^+ at 15-keV beam energy showed the ratio

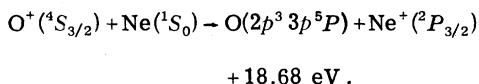
$$\text{O}^+:\text{N}^+:\text{Na}^+:\text{Mg}^+ = 1.0:0.7:0.4:0.2.$$

Andersen *et al.*¹³ have previously reported a similar dependence on these projectiles for outer-shell excitation of the $4p[\frac{3}{2}]$ level in NeI.

The ratio for the total photon yield indicates that the excitation of Ne may begin at a lower energy for an O^+ projectile than for a N^+ , Na^+ , or Mg^+ projectile. Measurements of the threshold values have confirmed this prediction. The threshold values were determined to be ~ 80 eV for O^+ , ~ 120 eV for N^+ , ~ 220 eV for Na^+ , and ~ 280 eV for Mg^+ projectiles with energies given in the laboratory system. The cross sections for excitation of the $3p$ levels in Ne rise sharply from the threshold values to reach maxima in the 1-2-keV region.

B. O^+ -Ne system

For the O^+ -Ne system, the excitation of the $3p$ levels in Ne was investigated together with the following charge-exchange reaction



The charge-exchange reaction leading to $\text{O}(\text{}^2p^3\text{}^3p\text{}^5P)$ with a ΔE value of 18.93 eV was also observed, but the 5P levels were much more populated than the 3P levels. No other excited oxygen levels occur within the energy region of interest, but higher-lying levels such as the $5s\text{}^5S$ and the $4d\text{}^5D$ levels were also observed to be populated, but only to a small extent compared with the population of the 5P levels.

The three $3p\text{}^5P$ levels decay at 7771-7774 Å to the $3s\text{}^5S$ levels in OI with a lifetime for the $3p\text{}^5P$ level of 29 nsec.¹⁴ With the present experimental apparatus, the correction for the lifetime of the 5P levels in the emission cross section accounts for less than 1%. The three 5P levels are so close lying that it has not been attempted to investigate them separately. The same is the case for the three 3P levels decaying at 8446 Å to the $3s\text{}^3S$ level with a 35-nsec lifetime.¹⁴

Figure 2 shows the emission cross sections for the $3p\text{}^5P$ levels in OI and for the $3p[\frac{5}{2}]_3$ level in

Ne. Strong oscillations, which are 180° out of phase, are observed. The oscillation maxima are equidistant on a v^{-1} scale within an accuracy of $\sim(5-10)\%$. The mean distance between the maxima is equal to $\Delta(v^{-1}) = (3.2 \pm 0.2) \times 10^{-8}$ sec/cm.

Within the energy region investigated, the emission cross sections for the eight $3p$ levels in Ne ranging from the $3p'[\frac{5}{2}]$ level at 18.53 eV to the $3p'[\frac{1}{2}]_1$ level at 18.72 eV exhibit the same number of maxima, which occur at the same velocities and with identical spacing between the maxima. In Fig. 3 the emission-cross-section curves are shown for the $3p'[\frac{1}{2}]_1$ level (18.72 eV), the $3p'[\frac{3}{2}]_1$ level (18.69 eV), and the $3p[\frac{5}{2}]_3$ level (18.55 eV).

The emission cross sections for the $3p[\frac{1}{2}]_1$ level (18.38 eV) and for the $3p'[\frac{1}{2}]_0$ level (18.96 eV) deviate from those of the other eight $3p$ levels. Figure 4 shows a comparison of the emission-cross-section curves for the $3p[\frac{1}{2}]_1$, $3p[\frac{5}{2}]_3$, and $3p'[\frac{1}{2}]_0$ levels. The number of oscillation maxima for the $3p[\frac{1}{2}]_1$ level corresponds to the number seen for the $3p[\frac{5}{2}]_3$ level, but the maxima are shifted towards lower velocities, whereas the mean distance between the maxima is the same within the experimental accuracy. For the $3p'[\frac{1}{2}]_0$ level, the maxima indicated by the arrows above the curve exhibit the same mean distance as observed for the other $3p$ levels, but the peaks are shifted towards higher velocities. Four additional peaks (indicated by arrows below the curve) are present in the emis-

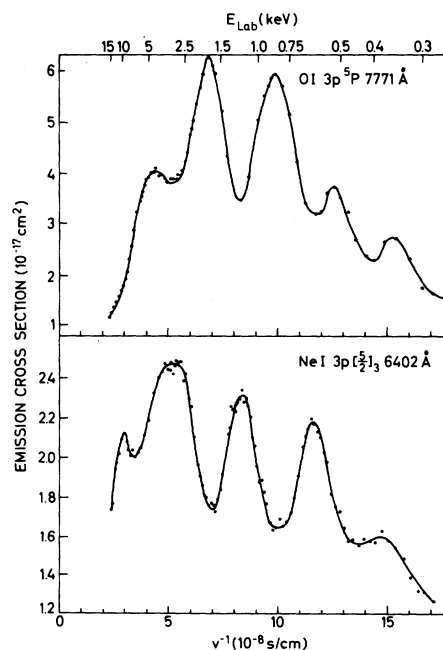


FIG. 2. Absolute emission cross sections for the production of 7771-Å OI ($3p\text{}^5P$) and 6402-Å NeI ($3p[\frac{5}{2}]_3$) radiation in O^+ -Ne collisions.

sion-cross-section curve, but these cannot be accounted for by interference with the charge-exchange process leading to the $3p^5P$ levels in OI.

The shift in the maximum positions for the $3p[\frac{1}{2}]_1$ level towards lower velocities cannot be accounted for exclusively by the cascade contribution from the $3d$ levels. The emission-cross-section curve for the $3d[\frac{3}{2}]_2$ level, which is responsible for the main cascading into the $3p[\frac{1}{2}]_1$ level at 7488 Å, is shown in Fig. 5. The cascade effect is not negligible, but the emission-cross-section curve for the $3d[\frac{3}{2}]_2$ level cannot explain why all four maxima on the emission-cross-section curve for the $3p[\frac{1}{2}]_1$ are shifted towards lower energies but keep constant the mean distance between the maxima. It should be born in mind that direct excitation of the $3p[\frac{1}{2}]_1$ level accounts for two thirds of the total population, whereas cascading accounts for only one third of the population of the $3p[\frac{1}{2}]_1$ level.

The four additional peaks observed on the emission-cross-section curve for the $3p'[\frac{1}{2}]_0$ level may be accounted for by interference between the charge-exchange channel leading to the $3p^3P$ levels in OI ($\Delta E = 18.93$ eV) and the direct-excitation channel leading to the $3p'[\frac{1}{2}]_0$ level in Ne I ($\Delta E = 18.96$ eV). The emission-cross-section curve for the $3p^3P$ levels in OI is shown in Fig. 6 together with arrows indicating the positions of the additional peaks on the emission-cross-section curve for the $3p'[\frac{1}{2}]_0$ level.

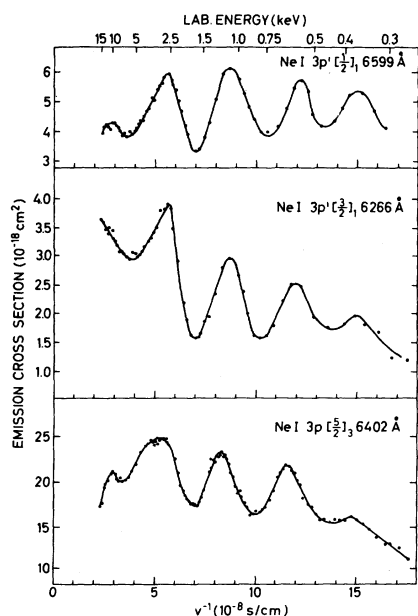


FIG. 3. Absolute emission cross sections for the production of 6599-Å Ne I ($3p'[\frac{1}{2}]_1$), 6266-Å Ne I ($3p'[\frac{3}{2}]_1$), and 6402-Å Ne I ($3p[\frac{3}{2}]_3$) radiation in O^+ -Ne collisions.

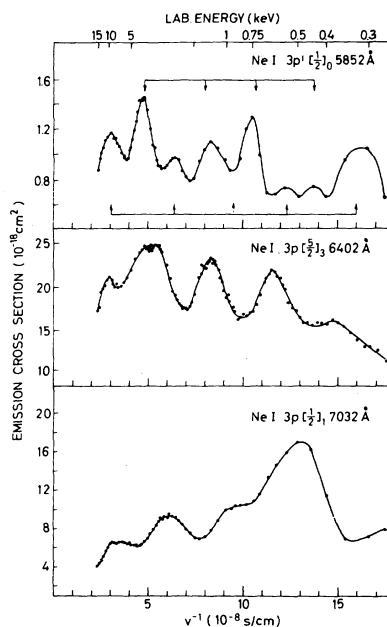


FIG. 4. Absolute emission cross sections for the production of 5852-Å Ne I ($3p'[\frac{1}{2}]_0$), 6402-Å Ne I ($3p[\frac{5}{2}]_3$), and 7032-Å Ne I ($3p[\frac{1}{2}]_1$) radiation in O^+ -Ne collisions.

The emission-cross-section curve for the $3p^3P$ levels in OI shows oscillations which are 180° out of phase with the additional peaks observed in the emission-cross-section curve for the $3p'[\frac{1}{2}]_0$ level in Ne I. Thus the direct-excitation channel leading to population of the $3p'[\frac{1}{2}]_0$ level in Ne interferes with the two charge-exchange channels leading, respectively, to the $3p^5P$ and $3p^3P$ levels in OI. Within the experimental accuracy, the mean distance between the maxima is the same for the

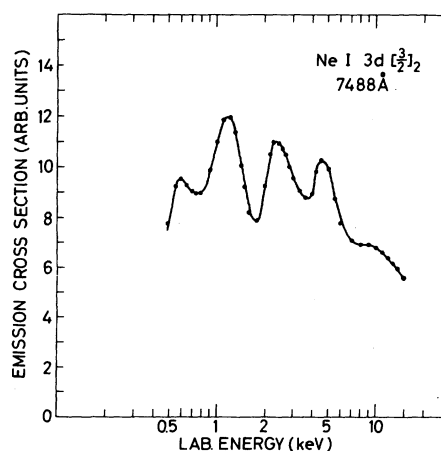


FIG. 5. Emission cross sections for the production of 7488-Å radiation from the $3d[\frac{3}{2}]_2$ level in Ne I in O^+ -Ne collisions. Emission cross section is given in arbitrary units.

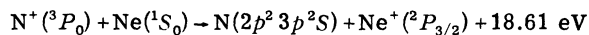
$3p^5P$ and $3p^3P$ data, i.e., $\sim 3.2 \times 10^{-8}$ sec/cm.

The polarization of the light emitted from the $3s$ - $3p$ transitions in Ne I with $J \neq 0$ for the upper levels, and from the $3s^5S$ - $3p^5P$ transition in O I was investigated. Energy-dependent polarization effects have been observed in the optical radiation emitted from the excited levels in Ne, particularly at 6266 Å, depopulating the $3p'[^3_2]_1$ level ($J=1 \rightarrow J=0$). Transitions depopulating $3p'[^3_2]_2$, $3p[^3_2]_1$, $3p[^5_2]_2$, and $3p[^5_2]_3$ levels all show polarization fractions ranging from ≈ 0 to 20%, whereas the light emitted from the $3p'[^1_2]_1$, $3p[^3_2]_2$, and $3p[^1_2]_1$ levels in Ne I and from the $3p^5P$ levels in O I showed a polarization fraction only ranging from 0 to 8%.

The oscillatory structure seen in the emission cross sections is also observed in the polarization-fraction data. This is illustrated in Fig. 7 for the Ne I, 6266-Å, $3p'[^3_2]_1$, $J=1$ to $J=0$ case, where the contributions to the cross sections of the two polarization components (appropriately weighted for intensity anisotropy) are shown along with the polarization-fraction data. The oscillatory structure in the emission cross section for the $3p'[^3_2]_1$ level is seen to be nearly exclusively due to the component of the emitted radiation polarized perpendicular to the incident-beam direction.

C. N^+ -Ne system

For the N^+ -Ne system, six charge-exchange processes have energy defects within the interval 18.0–19.2 eV. The energy defect ranges from 18.61 eV for the process



to 19.14 for the process leading to $N(2p^23p^2P)$.

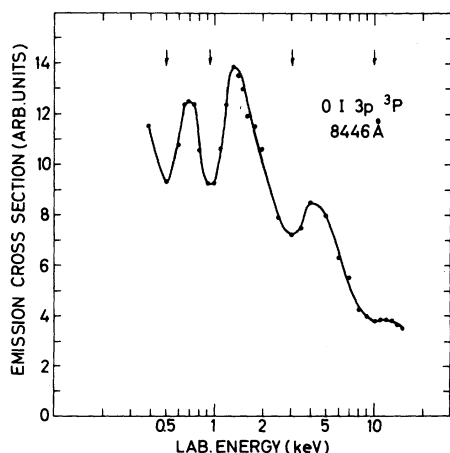


FIG. 6. Emission cross section for the production of 8446-Å radiation from the $3p^3P$ level in O I in O^+ -Ne collisions. Emission cross section is given in arbitrary units.

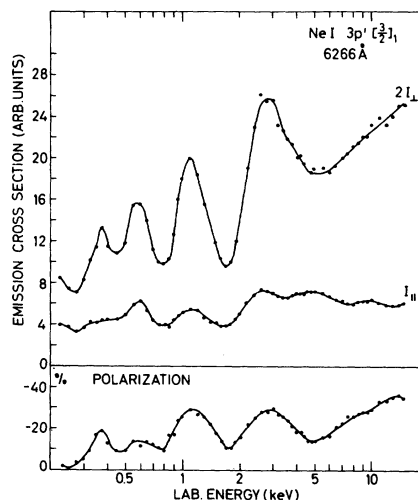


FIG. 7. Contributions of the two polarization components to the total emission cross section for the production of 6266-Å Ne I radiation from the $3p'[^3_2]_1$ level together with the polarization fraction as a result of O^+ -Ne collisions.

The wavelength region accessible for the determination of the emission cross sections limited the reactions to be studied to

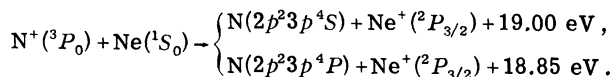


Figure 8 shows the emission cross sections for the $N(^4S)$ and the $3p[^3_2]_1$ levels in Ne. The oscillations are 180° out of phase. The oscillation maxima are equidistant on a v^{-1} scale within an accuracy of 10%. The mean distance between the maxima

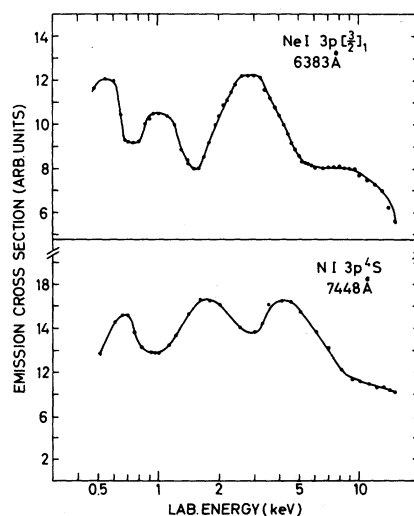


FIG. 8. Emission cross section for production of 7448-Å Ni ($3p^4S$) and 6383-Å Ne I ($3p[^3_2]_1$) radiation in N^+ -Ne collisions. Cross sections are given in arbitrary units.

is equal to $\Delta(v^{-1}) = (3.2 \times 10^{-8}) \pm (0.3 \times 10^{-8})$ sec/cm.

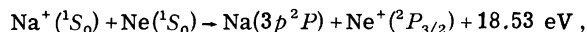
Table II lists the maxima positions for the emission-cross-section curves for the $3p'[\frac{1}{2}]_0$ level (18.96 eV), the $3p[\frac{3}{2}]_2$ level (18.63 eV), and the $3p[\frac{1}{2}]_1$ level (18.38 eV). The same trend as that observed for the O^+ -Ne system with respect to shifts in maxima positions is present for the N^+ -Ne system. The $3p[\frac{3}{2}]_2$ data are representative for the eight $3p$ levels ranging from 18.53 to 18.72 eV.

The emission-cross-section curve for the $3p^4P$ levels in NI exhibits maxima at 0.72, 1.50, and 4.65 keV, in good agreement with the peak positions for the $3p^4S$ levels (Fig. 8). A minor extra peak was observed at 2.70 keV.

Figure 9 shows that the oscillatory structure seen in the emission cross sections for the $3p'[\frac{3}{2}]_1$ level in Ne is due mainly to the component of the emitted radiation polarized perpendicular to the incident-beam direction. The polarization behavior for the other $J \neq 0$ levels in Ne was similar in magnitude and energy dependence as that seen for the O^+ -Ne system. The maxima positions of the two polarization components in Fig. 9 do not coincide with respect to beam energy. The dominant perpendicular component has its maxima at 0.57, 1.00, 2.50, and ~ 9.5 keV, whereas the parallel component has maxima at 0.62, 1.10, and 3.25 keV and no definite peak in the 9–11-keV region. It should be noted that both component curves show a tendency towards a shoulder in the region around 2.70 keV.

D. Na^+ -Ne system

For the Na^+ -Ne system, only one charge-exchange process, viz.,



should be taken into consideration. Figure 10 shows the emission cross sections for some $3p$ levels in Ne together with the data for the $3p^2P$ levels in Na. The positions of the maxima peaks near 2.8 and 9.0 keV are shifted slightly towards

TABLE II. Position of the oscillation maxima in N^+ -Ne collisions.

Level	Maxima position (keV)			
	I	II	III	IV
$3p'[\frac{1}{2}]_0$	0.75	1.30	3.50	10.0
$3p[\frac{3}{2}]_2$	0.58	1.05	2.75	9.0
$3p[\frac{1}{2}]_1$		0.62	2.40	7.2

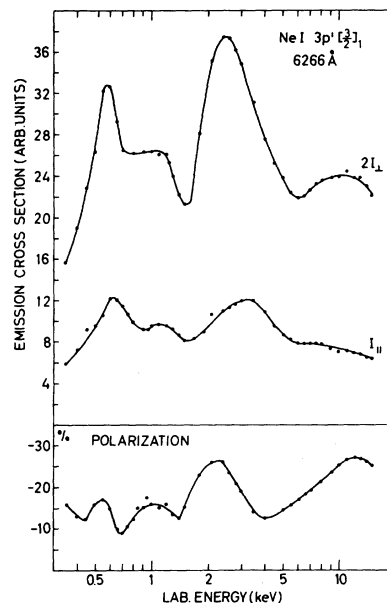


FIG. 9. Contributions of the two polarization components to the total emission cross section for the production of 6266-Å Ne I radiation from the $3p'[\frac{3}{2}]_1$ level, together with the polarization fraction as a result of N^+ -Ne collisions.

higher energies (3.2 and 11.0 keV) for the $3p'[\frac{1}{2}]_0$ level (Fig. 10) and towards lower energies (2.4 and 7.5 keV) for the $3p[\frac{1}{2}]_1$ level (not shown) in agreement with the observations for the O^+ -Ne and N^+ -Ne systems. The figure also shows that the

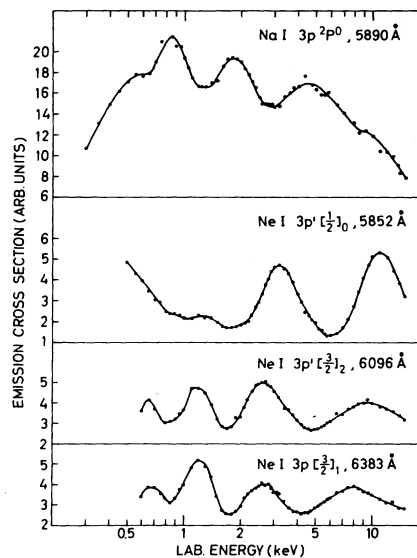


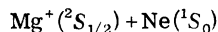
FIG. 10. Emission cross section for production of 5890-Å Na I ($3p^2P$), 5852-Å Ne I ($3p'[\frac{1}{2}]_0$), 6096-Å Ne I ($3p'[\frac{3}{2}]_2$), and 6383-Å Ne I ($3p[\frac{1}{2}]_1$) radiation in Na^+ -Ne collisions. Cross sections are given in arbitrary units.

intensity of the various peaks can shift from one level to the other. In a v^{-1} plot, the maxima for the $3p^2P$ levels in Na and for the $3p$ levels in Ne are equidistant and within an accuracy of 10%; the mean separation is $\Delta(v^{-1}) = 3.2 \times 10^{-8}$ sec/cm. While the spacing is nearly the same for all $3p$ levels in Ne, the present data show that the initial phase φ for $1/v \rightarrow 0$ will be different for the $3p'[\frac{1}{2}]_0$ and $3p'[\frac{1}{2}]_1$ levels and the other $3p$ levels in Ne.

Strong polarization was observed for the light emitted from some of the $3p$ levels in Ne, whereas the 5892-Å light from the $3p$ levels in Na was nearly nonpolarized. Figure 11 shows the contribution of the two polarized components to the emission cross section for the transition at 6266 Å depopulating the $3p'[\frac{3}{2}]_1$ Ne level. The strong oscillatory structure present in the emission cross section for the $3p'[\frac{3}{2}]_1$ level is due, nearly exclusively, to the polarization component perpendicular to the ion-beam direction. Tolk *et al.*⁸ have previously reported a similar effect, but with no oscillations present in the polarization component parallel to the beam direction.

E. Mg⁺-Ne system

Two charge-exchange reactions leading to excited states in neutral Mg have energy defects in the 18.0–19.2-eV energy interval:



$$\begin{cases} \text{Mg}(3p^1P_1) + \text{Ne}^+ (^2P_{3/2}) + 18.27 \text{ eV}, \\ \text{Mg}(4s^3S_1) + \text{Ne}^+ (^2P_{3/2}) + 19.03 \text{ eV}. \end{cases}$$

The Mg energy levels are located either below (18.27 eV) or above (19.03 eV) the $3p$ levels in Ne.

The emission cross sections measured for the population of the $3p'[\frac{1}{2}]_1$, $3p'[\frac{3}{2}]_2$, $3p[\frac{3}{2}]_2$, and $3p[\frac{3}{2}]_1$ levels all show oscillatory structures of the same spacing and phase with the oscillations 180° out of phase with the emission-cross-section oscillations observed for the $3p^1P_1$ level in Mg. Figure 12 illustrates this observation. The mean separation of the maxima has been determined in a v^{-1} plot to be $\Delta(v^{-1}) = 3.8 \times 10^{-8}$ cm⁻¹ sec. The emission curve for the $3p[\frac{1}{2}]_1$ level was similar to the ones just mentioned, but with peak positions shifted towards lower energies. For the $3p[\frac{5}{2}]_2$ and the $3p[\frac{5}{2}]_3$ levels, the oscillatory structure was more complicated. The dominant peak at ~1.75 keV (Fig. 11) in the $3p[\frac{3}{2}]_2$ -level emission-cross-section curve was split into two or three narrow-lying peaks.

The emission-cross-section curve for the $3p'[\frac{1}{2}]_0$ level was markedly different from the data obtained for the majority of $3p$ levels. The $3p'[\frac{1}{2}]_0$ -level

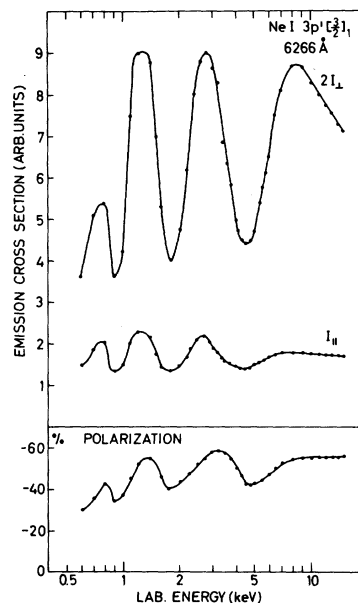


FIG. 11. Contribution of the two polarization components to the total emission cross section for the production of 6266-Å Ne I radiation from the $3p'[\frac{3}{2}]_1$ level together with the polarization fraction as a result of Na⁺-Ne collisions.

emission-cross-section curve was nearly in anti-phase with the emission cross section for, i.e., the $3p[\frac{3}{2}]_2$ curve. Figure 13 shows the emission-cross-section curve for the $3p'[\frac{1}{2}]_0$ level ($\Delta E = 18.96$ eV) in Ne together with the emission-cross-section

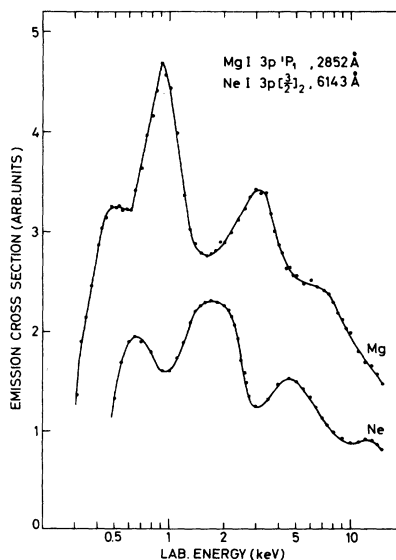


FIG. 12. Emission cross section for production of 2852-Å Mg I ($3p^1P_1$) and 6143-Å Ne I ($3p[\frac{3}{2}]_2$) radiation in Mg⁺-Ne collisions. Cross sections are given in arbitrary units.

curve for the $4s^3S_1$ level in Mg. The $4s^3S_1$ curve seems to consist of two oscillating systems. The dominant peak at 1.65 keV is assumed to belong to an oscillating system (indicated by arrows 1), which is in antiphase with the oscillations present in the emission-cross-section curve for the $3p'[\frac{1}{2}]_0$ level in Ne. A second oscillating system (indicated by arrows 2), which is in phase with the oscillations present in the $3p'[\frac{1}{2}]_0$ curve, is assumed to be due to the interference between the charge-exchange channel leading to the $4s^3S_1$ level in Mg and to the excitation channel leading to the population of the other nine $3p$ levels in Ne. The mean separation of the maxima in the $3p'[\frac{1}{2}]_0$ curve was determined in a v^{-1} plot to be 3.8×10^{-8} sec/cm.

The light emitted from the $3p^1P_1$ level in Mg and from the $3p'[\frac{3}{2}]_1$ level in Ne is strongly polarized, as shown in Figs. 14 and 15, respectively. The main contribution to the emission cross sections for both the $3p^1P_1$ level in Mg and for the $3p'[\frac{3}{2}]_1$ level in Ne comes from the emitted light polarized perpendicular to the beam direction, but the contribution from the parallel component is not negligible. The data show that the maxima on the curves for the two polarization components do not coincide for all peaks. It is noticed that the oscillations present in the polarization fraction for the $3p^1P_1$ level in Mg exhibit positive polarization below ~ 2 keV, but negative polarization above this energy.

For the Ne-polarization data, the three peaks all

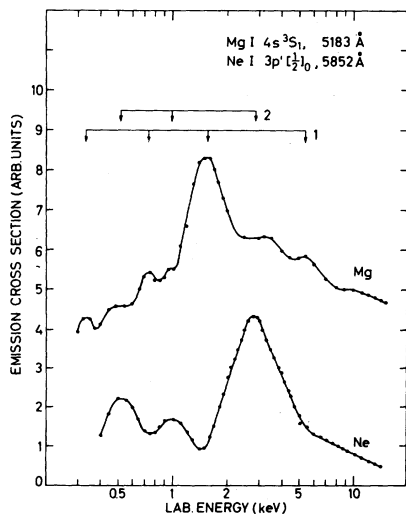


FIG. 13. Emission cross section for production of 5183-Å Mg I ($4s^3S_1$) and 5852-Å Ne I ($3p'[\frac{1}{2}]_0$) radiation in Mg^+-Ne collisions. Cross sections are given in arbitrary units.

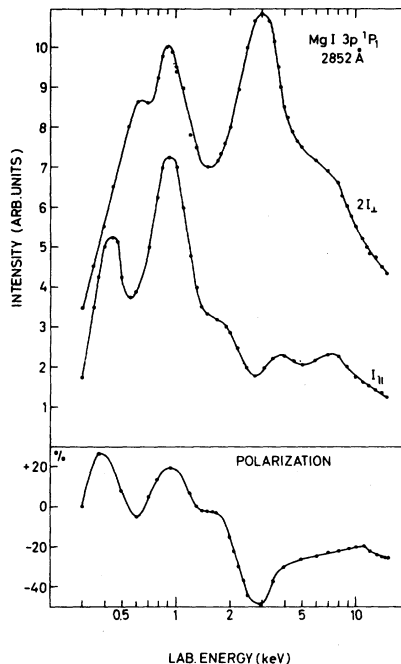


FIG. 14. Contributions of the two polarization components to the total emission cross section for the 2852-Å Mg I radiation from the $3p^1P_1$ level together with the polarization fraction as a result of Mg^+-Ne collisions.

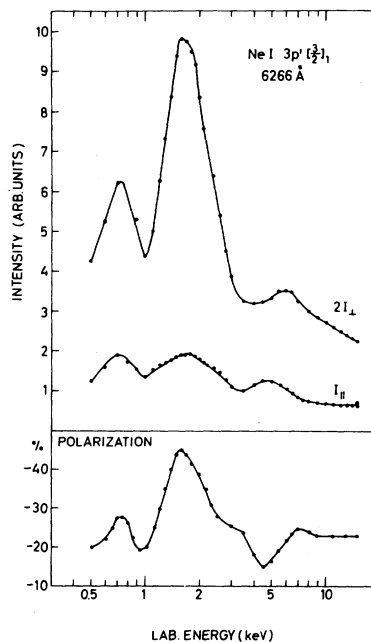


FIG. 15. Contributions of the two polarization components to the total emission cross section for the 6266-Å Ne I radiation from the $3p'[\frac{3}{2}]_1$ level together with the polarization fraction as a result of Mg^+-Ne collisions.

exhibit a negative polarization fraction. It should be noticed that the polarization fraction for the Ne data varies around the value -23% , and may be assumed to consist of two parts: an oscillating part showing a negative polarization fraction below ~ 3 keV, but positive above this energy; and a non-oscillating part with a negative polarization fraction of -23% over the energy region studied.

F. Weak or nonoscillatory systems

The Li^+ -Ne, Be^+ -Ne, and Al^+ -Ne systems all show a weak tendency towards oscillation in the emission cross sections for the $3p$ levels in Ne, but no regular oscillations as seen with the projectiles N^+ , O^+ , Na^+ , or Mg^+ were observed. Figure 16 shows the best resolved emission-cross-section curves obtained for the $3p$ levels in Ne, together with the results for the charge-exchange populated levels in Li ($2p^2P$, $\Delta E = 18.02$ eV), and Be ($3s^3S_1$, $\Delta E = 1870$ eV).

For the B^+ -Ne, C^+ -Ne, F^+ -Ne, or Ne^+ -Ne systems, the emission-cross-section curves for the $3p$ levels in Ne were smooth, and no tendency towards an oscillatory structure in the cross-section curves was observed.

III. DISCUSSION

A. Criteria for oscillatory structure

Phase-interference phenomena have so far been observed in systems with a charge on one of the collision partners in which the projectile and the target atoms had identical or homologous electron configurations [Na^+ -Ne,⁸ K^+ -Ar,³ Mg^+ -Rb,¹⁵ or Na^+ -He (Ref 4)], or they deviated from these configurations by only one electron [He^+ -He,¹ He^+ -Ne (Ref. 16)]. The conditions necessary for obtaining oscillatory structure in the total cross sections have been assumed to be⁴ (i) one of the collision partners should be an ion, (ii) the electronic configuration of the collision partners should be either identical or homologous or it should deviate with only one electron from these electronic configurations, and (iii) the energy levels of the pseudomolecular complex should be near degeneracy at large internuclear distance.

The recent observation by Kempter *et al.*⁶ of phase interference between two excitation channels leading to excited states in the projectile atom in collisions between 50- to 600-eV neutral potassium atoms and argon shows that a charge on one of the collision partners is not necessary for obtaining the oscillatory behavior of the total cross sections. The presence of strong regular oscillations in the total cross sections for the excitation and charge exchange in the systems N^+ -Ne and O^+ -Ne indicates

that the demand (ii) is not required and that quasimolecular interference may be expected in a rather large number of ion-atom or atom-atom collisions, i.e., also in ion-atom systems not exhibiting charge-exchange reactions.

Preliminary studies at this laboratory¹⁷ have shown strong regular oscillations 180° out of phase in the excitation cross sections for the 4^1D and 4^3D levels in He due to C^+ -He collisions. Since no charge-exchange reaction was observed in this system, the observed oscillations may represent phase interference between two quasimolecular excitation channels leading to the 4^1D and 4^3D levels in the target He, respectively.

The importance of the electronic configurations of the projectile and the target is noticed in the population of the various energy levels in the collision partners (Table I). The increased population of the $3p'[\frac{1}{2}]_0$ level and the reduced population of the $3p[\frac{5}{2}]_3$ level in Ne in the Na^+ -Ne system compared with the level population in the N^+ -Ne, O^+ -Ne, or Mg^+ -Ne systems show the important role of the electronic symmetry of the collision partners.

In the Li^+ -Ne system (homologous to the Na^+ -Ne system), the population of the $3p$ Ne levels follows the same trend as seen for the Na^+ -Ne system, but with a more dominant population of the $3p'[\frac{1}{2}]_0$ level, which is the strongest populated Ne $3p$ level in the Li^+ -Ne system.

Four of the eleven systems studied (B^+ , C^+ , F^+ ,

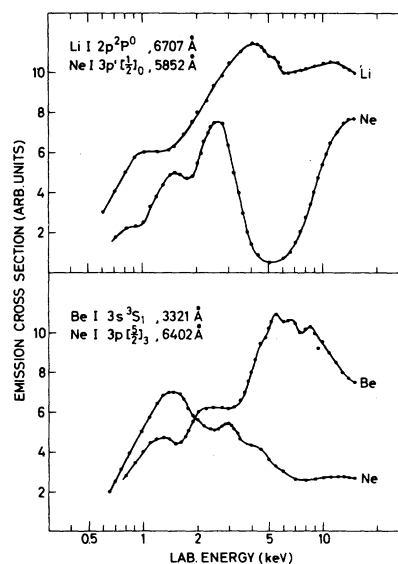


FIG. 16. Emission cross section for production of 6707-Å $\text{Li I } (2p^2P)$, 5852-Å $\text{Ne I } (3p'[\frac{1}{2}]_0)$, 3321-Å $\text{Be I } (3s^3S_1)$, and 6402-Å $\text{Ne I } (3p[\frac{5}{2}]_3)$ radiation in Li^+ -Ne and Be^+ -Ne collisions, respectively. Cross sections are given in arbitrary units.

Ne⁺) did not exhibit quasimolecular phase-interference effects. In the case of the B⁺-Ne and C⁺-Ne systems, the excited levels in BI and CI of interest for this study were not populated to any significant extent, and very few charge-exchange channels could be detected.

More than one set of reaction channels interact in the O⁺-Ne, N⁺-Ne, or Mg⁺-Ne systems, causing a more complex structure of the excitation or charge-exchange cross sections. Multiple interactions between the large number of charge-exchange channels (populating the close-lying energy levels in FI in the same energy region as that covered by the 3*p* levels in Ne) and the excitation channels leading to the excited 3*p* levels in Ne may perhaps account for the lack of oscillatory structure in the cross sections for the F⁺-Ne system.

In the Ne⁺-Ne system, the total cross section for excitation of Ne I 3*p* levels did not show oscillatory structure but exhibited the same structure as that seen for the Ne⁰-Ne collision system.⁴ A threshold value near 150 eV was followed by a fast rise to a maximum near 500 eV, from which energy the cross sections decreased monotonically to 15 keV. However, at energies below 1 keV it was not possible to separate the spectral lines due to the projectile from the spectral lines due to the target.

It is not possible from recent published data or from this investigation to establish the existence of a set of "selection rules" for the collision partners to be fulfilled to obtain phase-interference phenomena in low-energy atomic collisions. The formation of pseudomolecules seems at present to be so general that the "selection rules" will have to be very limited. More knowledge of the potential curves of the pseudomolecules to large internuclear distances seems essential for an understanding of the mechanisms responsible for inelastic processes in low-energy atomic collisions.

B. Comparison with theoretical predictions

The oscillatory structure present in the total cross sections has been explained by Rosenthal and Foley⁵ by a qualitative model, according to which coherent population of two energetically neighboring vacant quasimolecular terms occurs when the particles approach each other and a diabatic interaction between these terms follows, either as a result of term crossing or because of their close approach when the particles separate. Ankudinov *et al.*⁵ have attempted a more quantitative treatment on the basis of Rosenthal's original model. It is predicted by Ankudinov *et al.* that it should be possible to distinguish between term crossing and term approach from either the energy dependence of the modulation depth of the oscilla-

tions (the maximum depth of modulations is 50%) or from the initial-phase value Φ . It is assumed that the oscillatory part of the cross section in a v^{-1} plot can be described by a function of the type $(\text{const}) \times \cos(\mu_0/v + \Phi)$, where the period of oscillations is equal to $2\pi/\mu_0$.

In the case of term crossing, the modulation depth may decrease in the region of great velocities, and $\Phi \rightarrow \frac{1}{4}\pi$ for $v \rightarrow \infty$, whereas the modulation depth should be independent of velocity at large velocities and $\Phi \rightarrow 0$ for $v \rightarrow \infty$ for term approach. If the N⁺-Ne, O⁺-Ne, or Na⁺-Ne systems are considered, the modulation depth behaves identically for all ten 3*p* levels in Ne, but the initial-phase value Φ differs for the 3*p*' $[\frac{1}{2}]_0$, for the 3*p*' $[\frac{1}{2}]_1$, and for the eight 3*p* levels ranging from 18.55 to 18.72 eV, since Φ has been determined to be $\frac{1}{2}\pi$, 0, and π , respectively, for these three types of excitation curves.

Since the modulation behavior is the same for all the 3*p* levels in Ne at greater velocity although the initial phases differ, any conclusions drawn concerning the term behavior at large internuclear distances will be ambiguous. The present data suggest that new theoretical considerations are needed.

The magnitude of the oscillation period taken from experiments permits a determination of the area between the interfering quasimolecular levels³ by the relation

$$\text{area} = 2\pi \hbar / \Delta(v^{-1})$$

where $\Delta(v^{-1})$ is the distance between the oscillation maxima. The oscillation period is nearly identical for the N⁺-Ne, O⁺-Ne, Na⁺-Ne and Mg⁺-Ne systems, but previous studies³ also indicate a rather small change when passing from one system to another. The observation of identical oscillation periods for all 3*p* levels in Ne may perhaps indicate that the potential curves for all the pseudomolecular terms leading to excitation of Ne are nearly degenerate in the region reaching from the inner to the outer term crossing, at which distance the various atomic terms begin to split up according to their excitation energy.

C. Polarization data

On the basis of the molecular dual-coupling model suggested by Rosenthal and Foley⁵ and a molecular orbital-energy-level diagram based upon the promotion model,¹⁸ Tolk *et al.*⁸ have interpreted the oscillations present in the excitation curve for the 3*p*' $[\frac{3}{2}]_1$ level in the Na⁺-Ne system in the following way: Since the experimental polarization observations demonstrate that the atomic levels participating in the interference process are the $m = \pm 1$ sublevels and not the $m = 0$ levels, this in

turn implies that the molecular levels involved are the $\Omega = 1$ levels, where $\Omega = \Lambda + \Sigma$ is the azimuthal quantum number of the diatomic quasimolecule. The diabatic molecular orbital-energy-level diagram for the $(\text{NaNe})^+$ collision system, used by Tolk *et al.*, is shown in Fig. 17. The primary excitation mechanism may be due to a single pseudocrossing or a combination of pseudocrossings of the $3d\pi$ or the $4f\sigma$ incoming channels with the $5f\sigma$, $4d\pi$, $3p\pi$, and $4d\sigma$ levels.

A lack of interference at large nuclear distances between configurations of different values of the molecular-orbital quantum number is assumed. Thus, the problem is reduced to determining which of the MO pairs will interfere, the $5f\sigma$ - $4d\sigma$ pair or the $3p\pi$ - $4d\pi$ pair. Tolk *et al.*⁸ chose the $5f\sigma$ - $4d\sigma$ pair on the basis that the area enclosed by that pair was in better agreement with the experimentally determined value than the smaller area between the π molecular orbitals. This would indicate that the $5f\sigma$ - $4d\sigma$ interfering states are populated by an electron from the $3d\pi$ orbital.

It may be ambiguous to use as a selection criterion for the two sets of molecular orbitals the area enclosed by these molecular orbitals on Fig. 17. The two areas differ by less than $\sim 50\%$. The theoretical molecular-orbital curves are not calculated with such a high degree of accuracy that differences in the enclosed area of this order can be used as the only selection criterion.

If the $5f\sigma$ - $4d\sigma$ interfering states were responsible for the oscillatory behavior the population of these states should occur by an electron from the $3d\pi$ molecular orbital. There is no simple way to explain this population process, since the $3d\pi$ and the $5f\sigma$ - $4d\sigma$ curves do not cross. In contrast population of the $4d\pi$ - $3p\pi$ molecular orbitals from the $4f\sigma$ could account for the polarization data and the excitation process in a simple manner, since the $4f\sigma$ and the $4d\pi$ - $3p\pi$ terms do cross at an internuclear distance of ~ 1.0 a.u. Since the $4f\sigma$ term also crosses the $4d\sigma$ - $5f\sigma$ pair the oscillations seen in the I_{\parallel} component could also be accounted for by assuming that the $4f\sigma$ term is the electron-donating term.

Calculations of the distance of closest approach have been performed for the Na^+ -Ne system assuming a Lenz-Jensen or a Thomas-Fermi potential. The closest approach is assumed to occur in a head-on collision (scattering 180°). For the lowest energies at which the oscillation phenomenon is clearly detectable in the Na^+ -Ne system, ~ 0.5 keV, the distance of closest approach was determined to be 1.06 a.u. using the Lenz-Jensen potential, which normally gives too low values, and 1.24 a.u. using the Thomas-Fermi potential.

This calculation supports the hypothesis that the

population of the excited Ne levels occurs by the $4f\sigma \rightarrow 4d\pi$ - $3p\pi$ process. If the excitation mechanism was a transfer of an electron from the $3d\pi$ orbital to the $4d\sigma$ or $5f\sigma$ orbitals the most likely mechanism would involve either the $3p\pi$ or the $4s\sigma$ term crossing with the $3d\pi$ term, with subsequent transfer of the electron to the $4d\sigma$ - $5f\sigma$ pair. Crossings between the $3d\pi$ term and the $3p\pi$ - $4s\sigma$ terms only occur at internuclear distances ~ 0.35 a.u., which is considerably below the estimated value for closest approach.

The MO model may also be used to account qualitatively for the excitation mechanism in the N^+ -Ne, O^+ -Ne, and Mg^+ -Ne systems. In the case of the N^+ -Ne and O^+ -Ne systems the orbitals are arranged qualitatively as seen in Fig. 17, replacing Na with Ne and Ne with N or O, since the nl levels in N or O have less binding energy than in Ne. Thus the order of the energy levels will be $2s_{\text{Ne}} < 2s_{\text{N}} < 2p_{\text{Ne}} < 2p_{\text{N}}$. Excitation of a $2p$ electron in Ne to a $3p$ electron will have to occur by promoting the $2p$ electron from the $2p\pi$ or the $3d\sigma$ orbitals to the $5f\sigma$ - $4d\sigma$ or the $4d\pi$ - $3p\pi$ orbitals. It is suggested that the promotion occurs from the $3d\sigma$ to the $4d\pi$ - $3p\pi$ orbitals, since this orbital combination can account for the polarization data and the excitation mechanism in a simple manner owing to the crossing of the orbitals suggested, whereas this is not the case for the $2p\pi$ - $5f\sigma$ - $4d\sigma$ system.

It is likely that the molecular orbitals for the pseudomolecules $(\text{NNe})^+$, $(\text{ONe})^+$, and $(\text{NaNe})^+$ will be nearly identical with respect to the behavior of the orbitals of the excited states. Since the experimental data show that the area enclosed by the orbitals responsible for the oscillations are

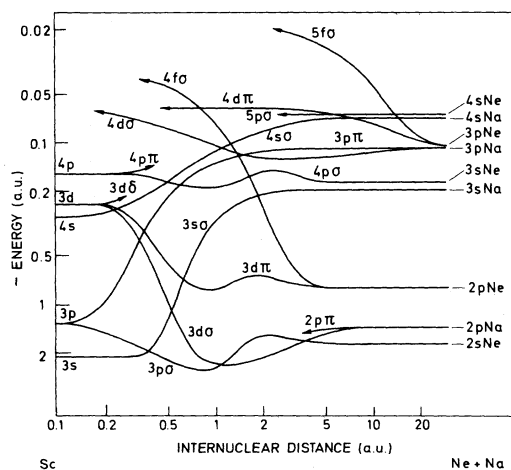


FIG. 17. Energy-level diagram of the diabatic molecular orbitals of the NaNe system. Energies are estimates based on the work on the Ne_2 system by E. W. Thulstrup and H. Johansen, *Phys. Rev. A* **6**, 206 (1972).

the same for these three pseudomolecular systems, it is suggested that the same pair of molecular orbitals is participating in all three systems. The $4d\pi-3p\pi$ pair seems to be the most likely one in the present case.

The polarization data for the Mg-Ne system can only be explained by assuming that two sets of molecular orbitals contribute to the oscillatory behavior. The marked change in the polarization behavior of the light emitted at 2852 Å from the $3p^1P_1$ state in Mg and at 6266 Å from the $3p^1[\frac{3}{2}]_1$ level in Ne can be explained by an energy dependence of the population of the two molecular-orbital pairs, the $5f\sigma-4d\sigma$ and $4d\pi-3p\pi$ pairs, which are respon-

sible for the observed oscillatory phenomena. The polarization measurements show that for the Mg^+-Ne systems the area enclosed by the $5f\sigma-4d\sigma$ or the $4d\pi-3p\pi$ pairs are nearly identical. Since the molecular orbitals for the excited levels in the $(NaNe)^+$ and $(MgNe)^+$ molecules may only differ slightly, the Mg^+-Ne data may support the hypothesis proposed for the oscillation behavior in the Na^+-Ne system.

ACKNOWLEDGMENTS

The authors thank the accelerator staff, particularly P. E. Christensen, for valuable assistance with the experiments.

-
- ¹D. Pretzer, B. van Zyl, and R. Geballe, *Phys. Rev. Lett.* **10**, 340 (1963); R. F. Stabbings, R. A. Young, C. L. Oxley, and H. Ehrhardt, *Phys. Rev.* **138**, A1312 (1965); M. Lipeles, R. Novick, and N. Tolk, *Phys. Rev. Lett.* **15**, 815 (1965); S. Dworetsky, R. Novick, W. W. Smith, and N. Tolk, *Phys. Rev. Lett.* **18**, 939 (1967), and references therein.
- ²H. S. W. Massey and E. H. S. Burhop, *Electronic and Ionic Impact Phenomena* (Clarendon, Oxford, 1952), pp. 513-14.
- ³S. Dworetsky, R. Novick, W. W. Smith, and N. Tolk, *Phys. Rev. Lett.* **18**, 939 (1967); S. V. Bobashev, in *Proceedings of the Seventh International Conference on the Physics of Electronic and Atomic Collisions, Invited Paper and Progress Report*, edited by T. R. Govers and F. J. de Heer (North-Holland, Amsterdam, 1972), pp. 38-64, and references therein; S. Bobashev, V. I. Ogurtsov, and L. A. Razumovskii, *Zh. Eksp. Teor. Fiz.* **62**, 892 (1972) [*Sov. Phys.—JETP* **35**, 472 (1972)].
- ⁴S. V. Bobashev and V. A. Kritskii, *Zh. Eksp. Teor. Fiz. Pis'ma Red.* **12**, 280 (1970) [*JETP Lett.* **12**, 189 (1970)]; N. H. Tolk, C. W. White, S. H. Dworetsky, and D. L. Simms, in *Proceedings of the Seventh International Conference on the Physics of Electronic and Atomic Collisions, Abstracts of Papers*, edited by L. M. Branscomb *et al.* (North-Holland, Amsterdam, 1971), pp. 584-86.
- ⁵H. Rosenthal and H. M. Foley, *Phys. Rev. Lett.* **23**, 1480 (1969); V. A. Ankudinov, S. V. Bobashev, and V. I. Perel, *Zh. Eksp. Teor. Fiz.* **60**, 906 (1971) [*Sov. Phys.—JETP* **33**, 490 (1971)].
- ⁶V. Kempter, B. Kübler, and W. Mecklenbrauck, *J. Phys. B* **7**, 149 (1974).
- ⁷T. Andersen, A. Kirkegård Nielsen, and K. J. Olsen, *Phys. Rev. Lett.* **31**, 739 (1973).
- ⁸N. H. Tolk, C. W. White, S. H. Neff, and W. Lichten, *Phys. Rev. Lett.* **31**, 671 (1973).
- ⁹O. Almén and K. O. Nielsen, *Nucl. Instrum. Methods* **1**, 302 (1957).
- ¹⁰G. Sørensen, thesis (University of Aarhus, 1973), pp. 22-26.
- ¹¹O. Poulsen, *Appl. Opt.* **11**, 1876 (1972).
- ¹²L. Wolterbeek Müller and F. J. de Heer, *Physica (Utr.)* **48**, 345 (1970).
- ¹³N. Andersen, K. Jensen, J. Jepsen, P. J. Martin, E. Veje, and A. M. Woolley, *Z. Phys.* **255**, 1 (1972).
- ¹⁴W. L. Wiese, M. W. Smith, and B. M. Glennon, *Atomic Transition Probabilities*, Nat'l. Bur. Std. Circ. No. 4 (U.S. GPO, Washington, D. C., 1968), Vol. I, and references therein.
- ¹⁵A. N. Zamilopulo, I. P. Zapesochnyi, G. S. Panev, O. A. Skalko, and O. B. Shpenik, *Zh. Eksp. Teor. Fiz. Pis'ma Red.* **18**, 417 (1973) [*JETP Lett.* **18**, 245 (1973)].
- ¹⁶N. H. Tolk, C. W. White, S. Dworetsky, and L. A. Farrow, *Phys. Rev. Lett.* **25**, 1251 (1970).
- ¹⁷T. Andersen, P. Hansen, and K. J. Olsen (unpublished).
- ¹⁸M. Barat and W. Lichten, *Phys. Rev. A* **6**, 211 (1972).